

Figure S1. **Efficient epidermis-specific deletion of aPKCλ in aPKCλ^{epi-/-} mice.** (A) Real-time RT-PCR analysis of aPKCλ and aPKCζ expression using RNA of newborn and P20 Ctr and aPKCλ^{epi-/-} mice. Data are presented as mean values ± SD; *n* = 5 mice/genotype; *, *P* < 0.05. (B) PCR analysis to genotype mice using aPKCλ-specific and K14-Cre-specific primers on genomic DNA isolated from tail biopsies showing the indicated genotypes with H₂O as a negative control. Wt, wild type; fl, floxed; del, deletion. (C) Real-time RT-PCR analysis of aPKCλ and aPKCζ on RNA isolated from P0 newborn and aPKCλ^{-/-} epidermis. *n* = 5 mice/genotype. Data are presented as mean values ± SD; *, *P* < 0.05. (D) Western blot analyses of Ctr and aPKCλ^{-/-} keratinocytes using an antibody recognizing total aPKCλ/ζ or phospho (p)-aPKCλ. Rac1 and GAPDH served as a loading control. (E) Immunofluorescence analysis of aPKCλ on P20 dorsal skin of Ctr and aPKCλ^{epi-/-} mice. Nuclei were counterstained with DAPI.

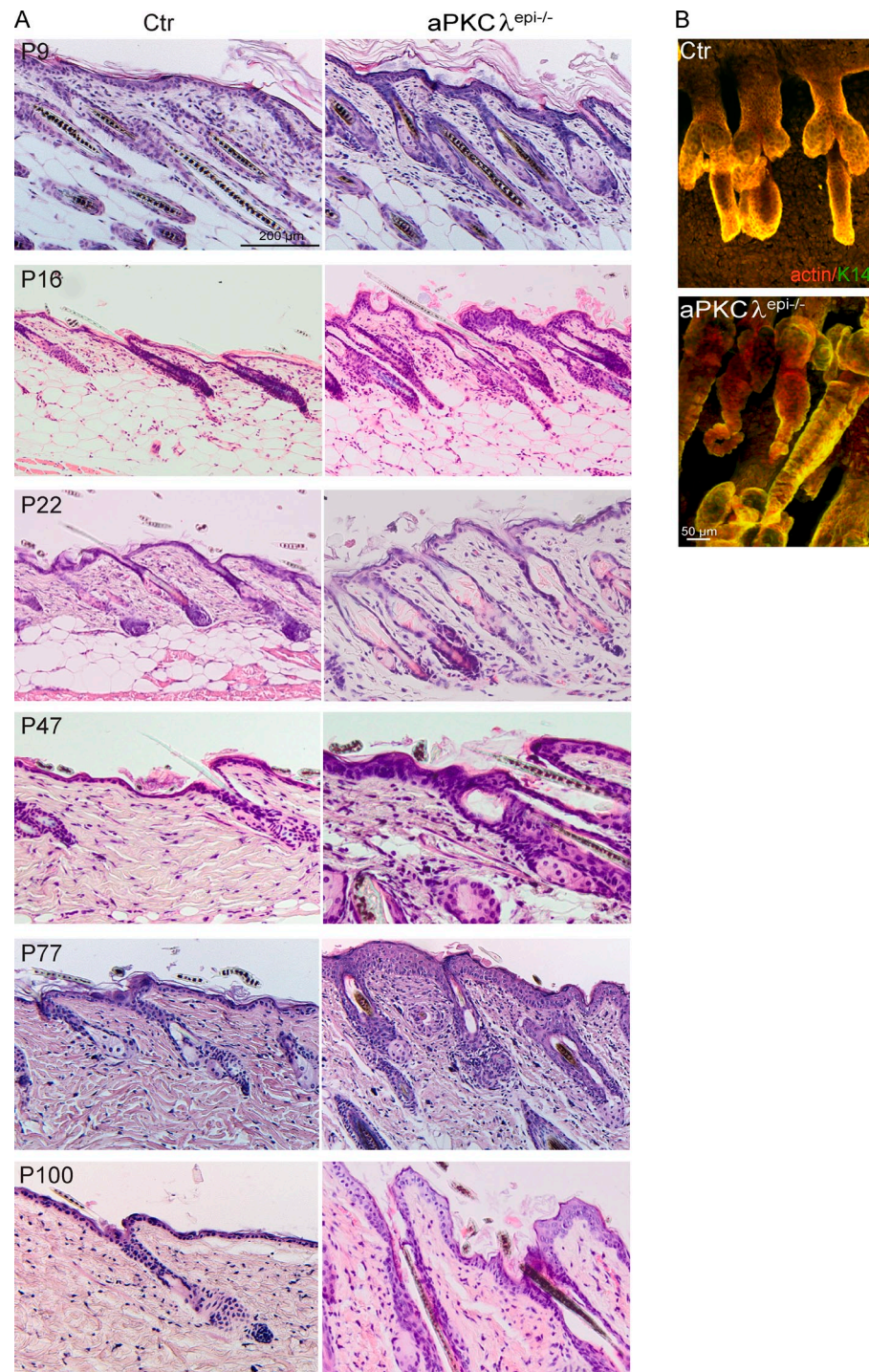


Figure S2. **Altered morphology of the epidermis and appendages upon loss of aPKCλ.** (A) Hematoxylin and Eosin staining of Ctr and aPKCλ^{epi-/-} paraffin back skin sections at the indicated postnatal days. (B) Whole-mount immunofluorescence analysis for keratin 14 (green) and actin (red) on tails from Ctr and aPKCλ^{epi-/-} mice at P58.

A

Name	Gene	Fold regulation	Specificity
K27	keratin complex-1, acidic, gene C29	-1,99	Medulla, IRS, Cuticle
K85	keratin complex 2, basic, gene 18	-2,32	Cuticle, Cortex
K2	keratin complex 2, basic, gene 17	-2,65	Upper epidermis /stratum corneum
K35	keratin complex 1, acidic, gene 24	-2,67	Cuticle
K82	keratin complex 2, basic, gene 20	-2,71	Cuticle
K71	keratin complex 2, basic, gene 6g	-2,77	IRS: Henle-, Huxley layer, cuticle
K32	keratin complex 1,acidic, gene 2	-3,39	Cuticle

B

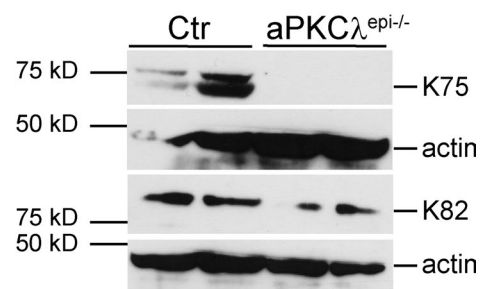


Figure S3. **Altered hair follicle differentiation in aPKC λ ^{-/-} mice.** (A) Selected Affymetrix global gene expression analysis of hair-specific keratin expression in Ctr and aPKC λ ^{epi-/-} newborn mice. (B) Western blot analysis of K75 and K82 using epidermal lysates from newborn Ctr and aPKC λ ^{epi-/-} mice. $n = 3$ mice/genotype. Western blot for β -actin served as a loading control.

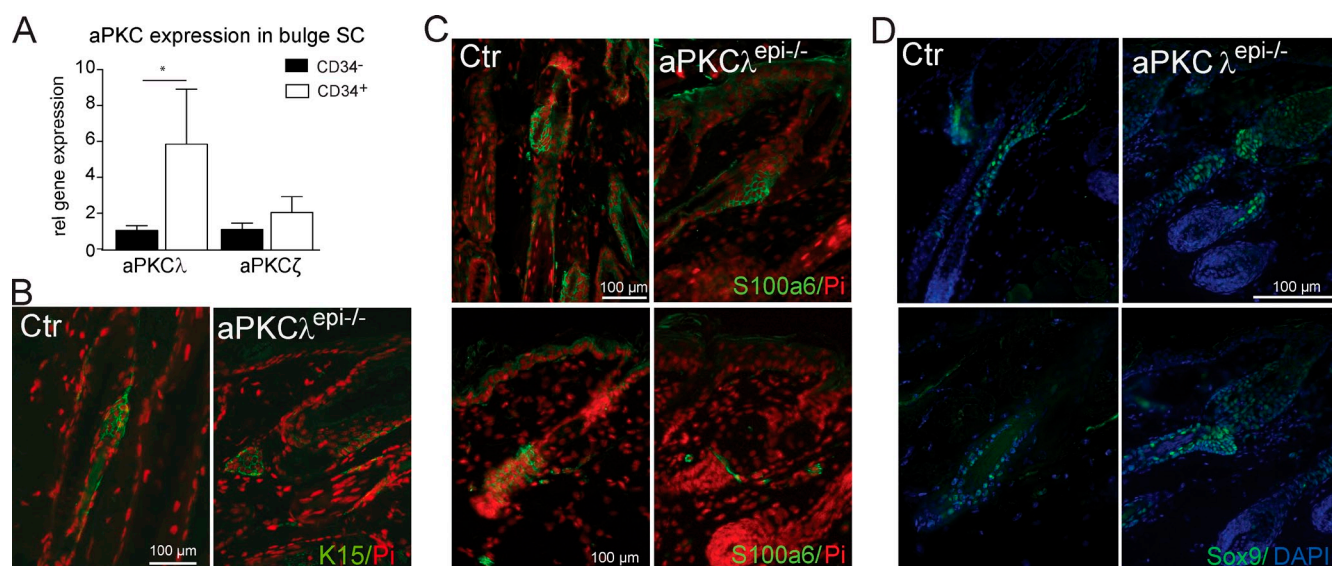


Figure S4. **Loss of bulge stem cell markers over time.** (A) Real-time PCR analysis for aPKC λ or aPKC ζ on FACS-sorted integrin $\alpha 6^+$ /CD34⁺ versus integrin $\alpha 6^+$ /CD34⁻ keratinocytes from adult Ctr mice (P33). $n = 7$ mice. Data are presented as mean values \pm SD; *, $P < 0.05$. (B) Immunofluorescence analysis of K15 on P33 dorsal skin sections. Nuclei were counterstained with propidium iodide (PI). (C) Immunofluorescence analysis of S100a6 on P33 (top) and P58 (bottom) dorsal skin sections of Ctr and aPKC λ ^{epi-/-} mice. Nuclei were counterstained with propidium iodide (PI). (D) Immunofluorescence analysis for Sox9 on dorsal skin sections of Ctr and aPKC λ ^{epi-/-} mice at P33 (anagen, top) and P77 (telogen, bottom). Nuclei were counterstained with DAPI.

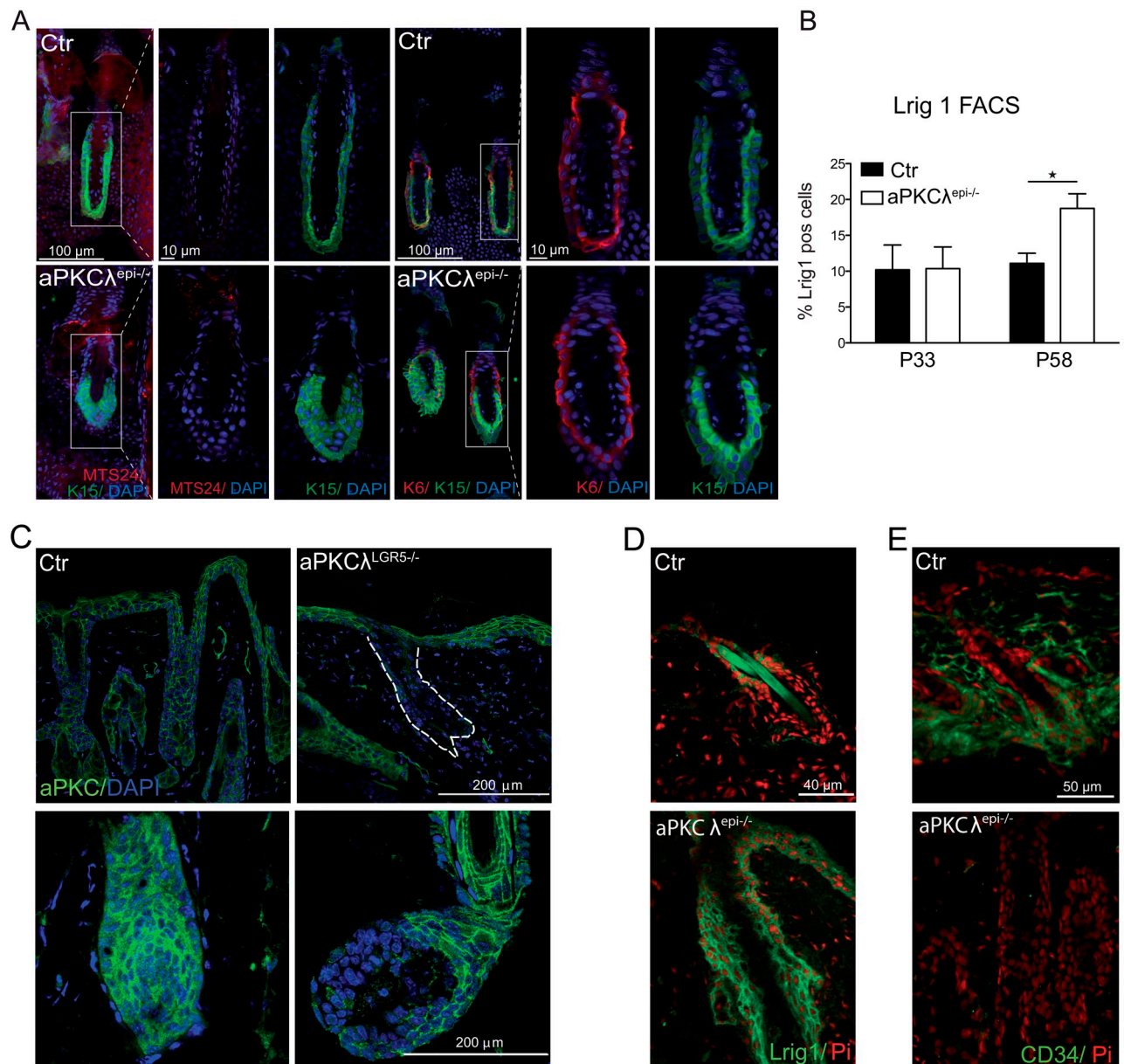


Figure S5. **Stem and progenitor cell changes upon loss of aPKC λ .** (A) Immunofluorescence analysis of either MTS24 and K15 (left six panels) or K6 with K15 (right six panels) on whole mounts of P33 tails isolated from Ctr and aPKC $\lambda^{epi-/-}$ mice. Nuclei were counterstained with DAPI. (B) Quantification of FACS analysis for Lrig1⁺ cells isolated from epidermis at P33 and P58. $n = 3$ mice/genotype/time point. Data are presented as mean \pm SD; *, $P < 0.05$. (C) Immunofluorescence analysis of aPKC on back skin sections of Ctr and aPKC $\lambda^{LGR5-/-}$ mice. Nuclei were counterstained with DAPI. (D and E) Immunofluorescence analysis of Lrig1 (D) or CD34 (E) on P365 back skin sections of Ctr and aPKC $\lambda^{epi-/-}$ mice. Nuclei were stained with propidium iodide (PI).

Table S1. **Antibodies**

Antigen	Source	Working Dilution	Catalogue Number	Company
Actin	Mouse	WB, 1:10,000	A3853; Lot: 6472J	Sigma-Aldrich
αPKCζ	Rabbit	IF, 1:200	Sc-216	Santa Cruz Biotechnology, Inc.
αPKCλ/ζ; thr 410/403	Rabbit	WB, 1:500	9378; Lot: F7	Cell Signaling Technology
BrdU	Mouse	IF, 1: 20	347580	BD
β-Catenin	Mouse	IF, 1:250; WB, 1: 2,000	610154	BD
CD34	Rat	IF, 1:50	553731	BD
CD34–Alexa 488	Rat	FACS, 1:25	553733	BD
CD43–Alexa 700	Rat	FACS, 1:25	560518	BD
Itga6/CD47f-PE	Rat	FACS, 1:30	555736	BD
K15	Mouse	IF, 1:1,000	MS-1068-P0	Thermo Fisher Scientific
K75	Guinea pig	IF, 1:2,000; WB, 1:4,000	GPK 6hf; Lot: 912040	Progen
K82	Guinea pig	IF, 1:2,000; WB, 1:2,000	GPhHa2; Lot: 906240	Progen
K85	Guinea pig	IF, 1:1,000	GP-hHb5; Lot: 802671	Progen
K28	Guinea pig	IF, 1:1,000	GP-K28; Lot: 802270	Progen
MTS24	Rat	IF, 1:50	/	A. Sonnenberg, Amsterdam, Netherlands
MTS24	Rat	IF, 1:100	/	R. Boyd, Melbourne, Australia
NfatC1	Mouse	IF, 1:50	SC-7294; Lot: D0708	Santa Cruz Biotechnology, Inc.
S100a6	Rabbit	IF, 1:1,000	RB-1805-A0; Lot: 1805A801F	Neomarkers
Sox9	Rabbit	IF, 1:150	SC-20095; Lot: H2808	Santa Cruz Biotechnology, Inc.
Survivin	Rabbit	IF, 1:400	2808; Lot: 71G4B7	Cell Signaling Technology

Table S2. **Microscopy**

Microscope (model; manufacturer)	Figure
Confocal microscope	
BX81; Olympus	2 A; 3 A, C, and E; 5 A, B, and G; 6 A, B, and K; 8 C; S5 A, C, D, and E
Meta LSM 510; Carl Zeiss	2 E; S2 B
Fluorescence microscope	
DeltaVision IX71; Olympus	2 B and C; S1 E; S4 B–D
Bright-field microscope	
DM4000B; Leica	1 B; 8 B; S2 A
BX51; Olympus	5 D and F
Electron microscope	
JSM-5910; JEOL	2 G